Simulations of fast switching between longitudinal modes of semiconductor laser cavity induced by on-chip filtered optical feedback

I. V. Ermakov,[1] S. Beri,[1,2] B. Docter,[3] J. Pozo,[3] M.K. Smit,[3] and J. Danckaert[1,2]

[1] Department of Applied Physics and Photonics, Vrije Universiteit Brussel
[2] Department of Physics, Vrije Universiteit Brussel
[3] COBRA Research Institute, TU Eindhoven

A set of delay differential equations is introduced to describe the multimode dynamics of a DBR laser cavity integrated with a passive filtered-feedback cavity. We demonstrate that a modulation of the central frequency of the feedback filter can be used to induce switches between different lasing modes of the DBR laser. The dependence on different model parameters such as feedback strength, feedback phase or cavity losses is quantitatively investigated.

Introduction

Nowadays tunable lasers (TL) are widely used in telecommunication networks since they allow for flexible reconfiguration in WDM systems, where a single TL can be used as a replacement for all fixed wavelengths lasers in the network [1]. In this paper we investigate switching dynamics of two longitudinal modes of Integrated Filtered-Feedback Tunable Laser (IFF-TL) based on a filtered feedback model.

Device and Model

A schematic picture of the novel IFF-TL is shown in Fig. 1. A Fabry-Perot (FP) laser is formed by a semiconductor optical amplifier (SOA) and two deeply etched DBR mirrors. The laser cavity length is chosen such that the mode spacing equals the channel spacing in the standard ITU-grid, e.g. 50 or 100 GHz. The FP laser is coupled to an Arrayed Waveguide Grating (AWG) filter that splits the light of the FP laser in several waveguide branches. Each branch contains an SOA that works as an optical gate. When the SOA is not biased it will absorb the light, but when put in forward bias the light will be transmitted or even amplified. The light is then reflected by another DBR mirror, and fed back through the AWG into the FP laser. The output light leaves the chip through the opposite DBR mirror.

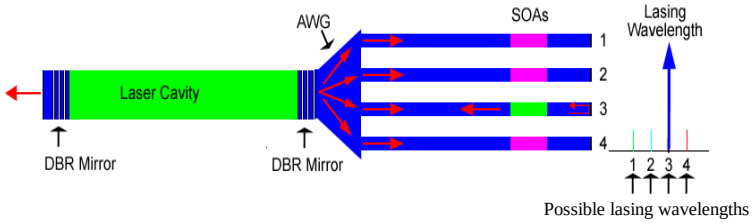

Fig. 1. Schematic picture of the IFF-TL device.

In order to demonstrate the operating principle, as well as testing the potential performance of the IFF-TL device, we performed numerical simulations based on an extended Lang-Kobayashi model [2,3]. This model consist of a set of coupled DDEs for the complex slowly varying field amplitudes E_m of each laser mode and an average

carrier inversion N [normalized at transparency N_0=1.5·10^8] in the FP cavity:

$$\dot{E}_m = \frac{1}{2}\cdot(1+i\alpha)\cdot\left[g(N(t)-N_0)\Big/\left(1+S|E_m|^2+C\sum_{k\neq m}|E_k|^2\right)-1/\tau_m^{ph}\right]\cdot E_m+\gamma_m F_m+f_E(t), \quad (1)$$

$$\dot{F}_m = \lambda E_m(t-\tau)e^{i\phi_m}+(i\Delta\omega_m-\lambda)F_m+f_F(t), \quad (2)$$

$$\dot{N} = \frac{I}{e}-\frac{N}{\tau_n}-g\cdot(N-N_0)\cdot\sum_{m=1}^{n}\left[|E_m|^2\Big/\left(1+S|E_m|^2+C\sum_{k\neq m}|E_k|^2\right)\right], \quad (3)$$

where α = 5 is the linewidth enhancement factor of the semiconductor material, τ_m^{ph} is the photon lifetime for mode m and g = 1.5·10^{-5} ns^{-1} is the differential gain. Different modes in the cavity are coupled nonlinearly by saturation processes such as spectral hole burning that are modeled here by the coefficients $S = C = 5\cdot10^{-7}$. Spontaneous emission of photons is modeled by Gaussian white noise terms $f_E(t)$ and $f_F(t)$ in Eqs. (1-2). Other parameters are: I = 45 mA is the injection current, τ_n = 2 ns is the carrier lifetime.

The feedback terms are given by strengths γ_m, phases ϕ_m and delay times $\tau = 2L_{ext}N_g/c$ ≈ 46.2 ps, where L_{ext} ≈ 1.9 mm is the length of external branches, N_g ≈ 3.65 is the group index of the waveguide, c is the speed of light in vacuum. The feedback cavity is modeled as a Lorentzian filter with half width at half maximum λ = 200 GHz and detuning $\Delta\omega_m$ = 0 as described by (2) for the auxiliary dynamical variables F_m.

Feedback Strength

Different bias currents on the SOAs can be modeled by feedback strength γ:

$$\gamma = \left((1-R_{DBR})/\tau_{in}\right)\cdot\sqrt{R_{DBR}^{ext}/R_{DBR}}\cdot(1-A_{DBR})^2\cdot {T_{AWG}}^2\cdot {A_{SOA}}^2, \quad (4)$$

where R_{DBR} is the reflectivity of an ideal DBR mirror of the main cavity. The scattering losses of the DBR mirrors are accounted for in an absorption term A_{DBR}. For the 2-period DBR mirror, which simulated reflection and transmission spectra are given in Fig. 2, A_{DBR} is given by $1\text{-}T_{DBR}/(1\text{-}R_{DBR})$ = 1-0.2/0.3 = 0.33. $\tau_{in} = 2L_{cav}N_g/c$ = 20 ps is the roundtrip time of the main cavity, R_{DBR}^{ext} is the reflectivity of the 3-period DBR mirror at the end of a feedback branch. T_{AWG} is the transmission of the AWG and A_{SOA} is the amplification of an SOA. In Fig. 3 we show the dependence of feedback strength γ on the amplification of an SOA for two types of DBR. We can see that a lower DBR reflectivity leads to a larger feedback signal, which is beneficial for the switching speed.

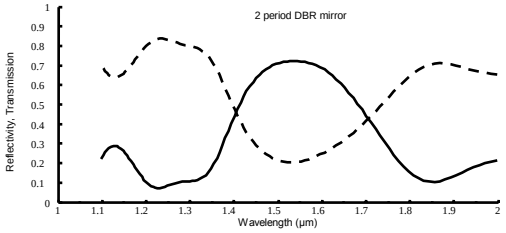

Fig. 2. Simulation of reflection (solid)/ transmission (dashed) of a 2 period deeply-etched DBR mirror.

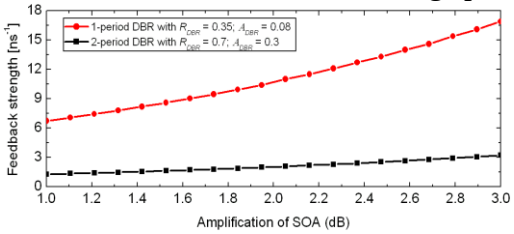

Fig. 3. Dependence of feedback strength γ on SOA amplification. R_{DBR}^{ext} = 0.85, T_{AWG} = 0.316.

Switching Dynamics of Two Modes

We illustrate the result in the simple, but not trivial case of two competing lasing

modes of the FP cavity. Each of them corresponds to a different AWG channel. Since we assume a flat gain spectrum, the lasing mode is selected by applying the feedback.

We induce mode-switching by alternating the feedback parameters γ_1 and γ_2 between 0.0 and 6.0 ns^{-1} in a pseudo-random way. Practically this corresponds to forward biasing one of the SOA gates without biasing the other gates. Eqs. (1-3) are solved using Runge-Kutta method of the second order with a fixed time-step of 10^{-5} ns.

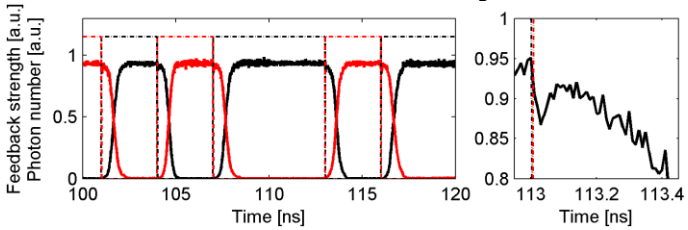

Fig. 4. Numerical simulations of a switching sequence induced by modulation of the feedback parameters. Solid lines: power in mode 1 and mode 2, dashed lines: feedback strength in channel 1 and channel 2. The image on the right shows a detail of the switching dynamics, where the drop in output power is visible when the feedback is switched. Parameters are $\gamma_1 = \gamma_2 = 0$ - 6 ns^{-1}, $\phi_1 = \phi_2 = 0$, $\tau_1^{ph} = 1.999\,ps, \tau_2^{ph} = 2\,ps$.

Time series of the mode-resolved power from simulations of Eqs. (1-3) are shown in Fig. 4. The device lases stably in one mode when the corresponding gate is forward biased. When the feedback is moved to the other channel, the operation switches to the other mode due to increase of the effective gain. The modal power rises and quenches the gain of the other mode. An evidence for this mechanism is the presence of a power drop in the time-series (see Fig. 4, right).

The dependence of the switching time on the feedback strength is shown in Fig. 5. Here we assumed that a switch is completed once the mode power reaches 90% of the total power. An average of 10 switches is used to calculate switching time.

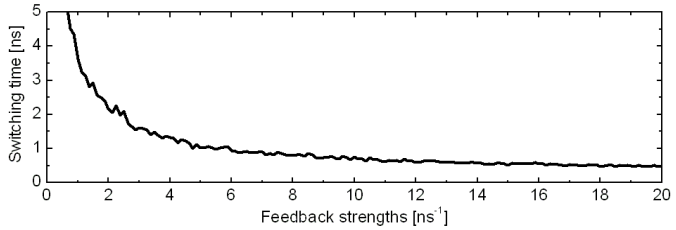

Fig. 5. Switching time versus the feedback strengths $\gamma_{1,2}$, $\phi_1 = \phi_2 = 0$, $\tau_1^{ph} = 1.999ps, \tau_2^{ph} = 2ps$.

As expected, an increase in the feedback intensity leads to a decrease of the switching time as the difference between the effective gains of the modes increases. The order of magnitude of the switching speed is in accordance with the measured switching speed of the ring resonator based filtered feedback devices presented in [4].

Phase Dependence and Effective Losses

The dependence of the switching time on the feedback phase is shown in Fig. 6.

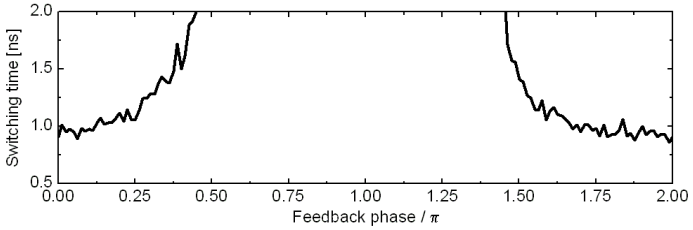

Fig. 6. Switching time versus the feedback phase ϕ_2, $\phi_1 = 0$, $\gamma_1 = \gamma_2 = 0$ - 6 ns^{-1}, $\tau_1^{ph} = 1.999ps, \tau_2^{ph} = 2ps$.

From Fig. 6 it is clear that no switches are observed for feedback phases between 0.5π and 1.5π, because when the feedback field is out-of-phase with the lasing mode, the effective gain decreases, leading to a suppression of the side mode instead of a switch.

The phenomena observed in Fig. 6 can be explained as follows. From simulations we observe that the two fields E_m and F_m are connected with a constant complex number A_m, i.e. $F_m = A_m \cdot E_m$. For the chosen parameters the system resides at a fixed point that can be found solving Eqs. (1-3) in the form: $E_m(t) = P \cdot e^{i\omega t}$, $F_m(t) = A_m \cdot P \cdot e^{i\omega t}$, $N(t) = Q$, where P, Q and ω are the real constants. The expressions for A_m and ω then read:

$$A_m = \lambda \cdot e^{i\phi_m - i\omega\tau} \Big/ (i\omega + \lambda), \tag{5}$$

$$i\omega = -0.5\left[(1+i\alpha)/\tau_m^{ph} - 2\gamma_m \lambda \cdot e^{i\phi_m - i\omega\tau} \Big/ (i\omega + \lambda) \right] + 0.5(1+i\alpha)\left(g(N - N_0)\right). \tag{6}$$

Effective losses are given by the term in the square brackets in Eq. (6), whose real part can be written as a function of feedback phase:

$$\mathrm{Re}\left(\Gamma_m^{eff}(\phi_m)\right) = 1/\tau_m^{ph} - 2\gamma_m \frac{\lambda^2 \cos(\phi_m - \omega\tau) + \lambda\omega \sin(\phi_m - \omega\tau)}{\omega^2 + \lambda^2}. \tag{7}$$

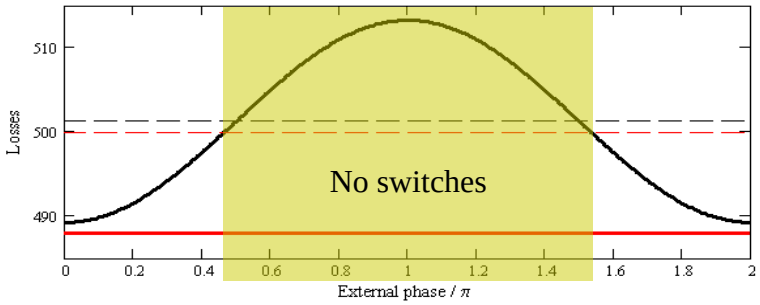

Fig. 7. Losses vs. feedback phase ϕ_2. Effective losses, induced by feedback light (solid) and losses without feedback (dashed). Parameters are $\phi_1 = 0$, $\gamma_1 = \gamma_2 = 6$ ns^{-1}, $\tau_1^{ph} = 1.999\text{ps}, \tau_2^{ph} = 2\text{ps}$.

In Fig. 7 we plot effective losses (solid) and loses given by photon lifetime (dashed) for both modes (black and red). When solid line crosses the dashed one the switches stop because effective losses of one mode (black) become higher that the losses of the other mode without feedback (red). The interval where switches are not observed is the same to the one obtained numerically and represented in Fig. 6. In the current design, therefore, the bias currents on the SOA gates can be used to influence the phase of the feedback light, since an increase in carrier density will lead to a change in refractive index. It is therefore possible to adjust the currents such that the feedback phase is in the necessary interval. Note that the exact current setting is therefore very tolerant.

References

[1] L. A. Coldren, "Monolithic tunable diode lasers," IEEE J. Sel. Topics in Quantum Electronics, vol. 6, 988-999, 2000

[2] R. Lang, K. Kobayashi, "External optical feedback effects on semiconductor injection laser properties," IEEE Journal of Quantum Electronics, vol. 16, 347-355, 1980.

[3] M. Yousefi, D. Lenstra, "Dynamical behavior of a semiconductor laser with filtered external optical feedback," IEEE Journal of Quantum Electronics, vol. 35, 970-976, 1999.

[4] S. Matsuo, T. Segawa, T. Kakitsuka, T. Sato, R. Takahashi, H. Suzuki, B. Docter, F. Karouta, M.K. Smit, "Integrated filtered feedback tunable laser using double-ring-resonator-coupled filter," IEEE 21st International Semiconductor Laser Conference, 2008. ISLC 2008, 155-156, 2008.